Effect of Plastic Deformation of Artificial Wedges on Fatigue Crack Closure

D.L. Chen
Department of Mechanical and Industrial Engineering, Ryerson University
350 Victoria Street, Toronto, Ontario M5B 2K3, Canada
Email: *dchen@ryerson.ca*

Abstract

Fatigue crack closure concept has been used to extend fatigue life of cracked components via slowing down or halting crack propagation by introducing a variety of artificial closure materials into the crack. This necessitated the consideration of deformation characteristics of the closure materials. The previously proposed elastic wedge closure model along with a modified partial crack closure concept was briefly reviewed. The elastic wedge model was then extended to integrate with the plastic deformation characteristics of the wedge based on the Ramberg-Osgood type relationship. The occurrence of wedge plasticity was observed to cause a non-linear concave variation in the applied stress-crack opening displacement (COD) response and the slope became smaller in comparison with the elastic wedge. This resulted in a greater effective stress range $\Delta\sigma_{eff}$ due to a larger COD range experienced by the fatigue crack tip for a given cyclic loading condition.

1. Introduction

Fatigue crack closure, initially discovered by Christensen [1] and defined by Elber [2], has been widely used to explain the effect of microstructure, environment, specimen thickness, stress ratio, overload, etc., on the fatigue crack propagation (FCP) behavior of materials, as documented in several overview papers and some recent publications, e.g. [3-12]. One of the practical applications involving fatigue crack closure is to slow down or halt FCP by deliberately infiltrating foreign materials into a crack, e.g. [13-15]. To overcome the shortcoming of conventional crack closure concept, which has been pointed out by a number of researchers, e.g., [4,16-21], a modified partial crack closure concept was proposed where the effect of the loading cycle below K_{op} on FCP has been taken into account [22-27]. The modified closure model [25] has been used to predict the improvements in the FCP life in AISI 4130 low alloy steel filled with artificial closure materials via plating on the cracked surfaces [13]. Through introducing artificial closure materials into fatigue cracks in 7075-T651 aluminum alloy sheet [28], 7050 aluminum alloy [29], AISI 304 stainless steel [14], JIS SM490A steel [15], etc., an effective FCP retardation effect was observed to occur, giving rise to a significant extension of fatigue life. This is due to the fact that the infiltrated wedge results in a premature contact of crack surfaces, leading to a smaller effective FCP driving force.

Since a variety of artificial closure materials with different deformation characteristics, such as electroless nickel [13,30], ethylcyanoacrylate adhesive [30], low-melting point solder [30], epoxy resin [14,29], alumina paste [15], have been used to retard the FCP, the plastic deformation of the artificial closure materials is expected to occur in some cases. This study is thus aimed at evaluating the effect of the plastic deformation of infiltrated wedge on the applied stress-COD behavior, based on the crack closure model [25]. To have a better understanding on the subsequent formulation, the main points in the original elastic wedge model [25] are briefly summarized as follows.

2. Elastic wedge closure model [25]

2.1 Closure-free crack

Based on linear elastic fracture mechanics (LEFM) the relationship between the externally applied stress, σ, and the crack opening displacement (COD), δ, of a crack of length, $2a$, in a center-cracked tensile specimen can be expressed as:

$$\sigma = k\delta \ , \tag{1}$$

$$k = \frac{E'}{4Y\sqrt{a_m(2a - a_m)}} \ , \tag{2}$$

where k is the slope of the applied stress-COD relationship in the closure-free case, a_m is the distance from the crack tip to an measuring location (Here a_m is used to replace the symbol a_i in [25]), Y is the geometric correction factor. $E' = E$ for plane stress, and $E' = \dfrac{E}{1-\nu^2}$ for plane strain, where E is the Young's modulus and ν is Poisson's ratio of the specimen material. Eqn (1), representing the applied stress-COD behavior in the closure-free case, denotes a straight line passing through the origin of the coordinates (δ=0, σ=0), suggesting that the crack faces are fully closed when the externally applied stress is removed.

2.2 Closure-affected crack

A model representing the presence of crack closure was proposed [25]. An elastic wedge inserted into the crack, with a width W_1 and height h_1, is located at a distance a_1 from the crack tip. It is used to simulate the roughness-/asperity- or oxide-induced closure. The same loading condition as that for the closure-free crack is applied to a CCT specimen containing a crack of length *2a* (specimen width W and thickness t). When the applied stress is higher than the opening (or closure) stress σ_{op} during unloading from the maximum applied stress σ_{max}, the applied stress-COD behavior is identical to that for the closure-free crack, i.e., Eqn (1) holds true, since the top side of the wedge does not contact the upper face of the crack in this stage (called stage I, as indicated in Fig.1).

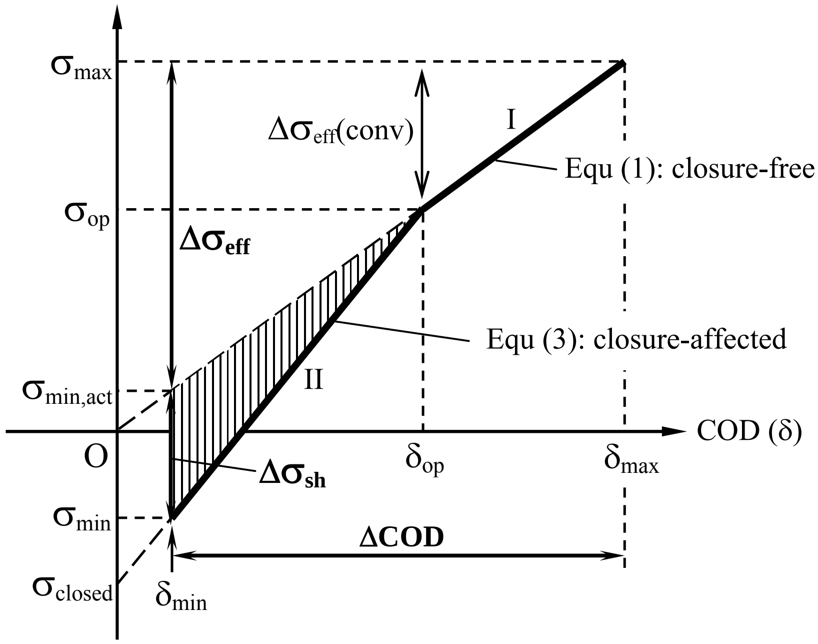

Figure 1 The applied stress-crack opening displacement (COD) behavior for the closure-free crack and closure-affected crack, showing the conventionally defined effective stress range, $\Delta\sigma_{eff}$(conv), and the modified definition of the effective stress range, $\Delta\sigma_{eff}$, which corresponds to ΔCOD experienced by the fatigue crack tip [25].

After the applied stress is unloaded below $\sigma_{op,}$ the wedge gets into touch with the crack face and resists the closing of the crack. The relationship between σ and δ in the closure-affected case has been derived to be [25],

$$\sigma = k(1+\lambda_1)\delta - \lambda_1 \sigma_{op} , \tag{3}$$

$$\sigma_{op} = \frac{h_1 E'}{4Y\sqrt{2\,a\,a_1}} , \tag{4}$$

$$\lambda_1 = \frac{8E_1 W_1}{\pi h_1 E'} . \tag{5}$$

The parameter, λ_1, proportional to the ratio of the Young's modulus of the wedge (E_1) to that of the specimen material (E) and pertinent to the stress state of the specimen (indicated by E'), could be considered to reflect the fracture surface topography by the wedge parameters (W_1 and h_1). It should be noted that λ_1, instead of λ in [25], is used here for the single-wedge case, since the multi-wedge cases have been taken into consideration [27]. The one-wedge model could be thought of representing a collective action of multiple-wedge contacts in a statistical sense. By setting (a) λ_1=0, (b) λ_1 equal to a finite value, and (c) $\lambda_1 \rightarrow \infty$ in Eqn (3), three types of the applied stress-COD behavior can be theoretically identified, as shown in Fig.2, corresponding to the long-established LEFM (flat crack plane and no closure), partial closure/shielding [3,22-27,31], and complete closure/shielding of the conventional closure concept, respectively.

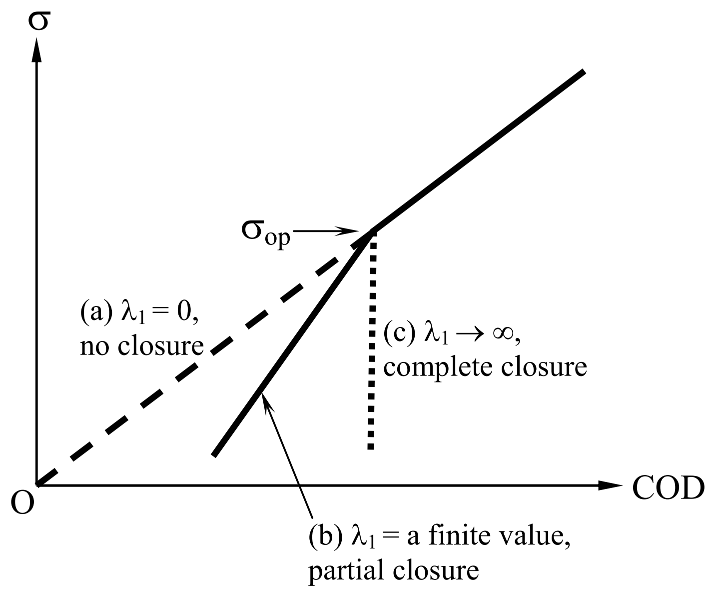

Figure 2 Three types of the applied stress-COD behavior [25]. (a) The closure-free case based purely on linear elastic fracture mechanics – flat crack surface and no closure, (b) the general case of partial closure (or partial shielding), (c) the extreme case of complete closure/shielding based on the conventional crack closure concept.

Based on the consideration that FCP is governed by the near-tip crack opening displacement range (ΔCOD), the fatigue crack closure effect has been re-defined via comparing the applied stress-COD behavior in the closure-affected case with that in the closure-free case. Two key parameters were then defined [22-26] and are shown in Fig.1. One is the maximum *sh*ielding stress intensity *range* for a given cyclic loading (ΔK_{sh}), the other is the *min*imum local (or tip) stress intensity factor *act*ually transmitted to the crack tip ($K_{min,act}$) at the minimum applied stress σ_{min}. In terms of Eqns (1) and (3), ΔK_{sh}, $K_{min,act}$ as well as K_{op} can be derived to be,

$$\Delta K_{sh} = \frac{\lambda_1}{1+\lambda_1}\left(K_{op} - K_{min}\right), \tag{6}$$

$$K_{min,act} = \frac{1}{1+\lambda_1}\left(\lambda_1 K_{op} + K_{min}\right), \tag{7}$$

$$K_{op} = \frac{h_1 E'}{8}\sqrt{\frac{2\pi}{a_1}}, \tag{8}$$

where K_{min} and K_{op} are the applied minimum stress intensity factor and crack opening stress intensity factor, respectively. Eqn (8) was found to lie in-between Suresh and Ritchie's equation [32] and Beevers *et al.*'s equation [33], with a proportion of $2/\pi:1:2$ for Suresh and Ritchie [32], ours [25], and Beevers *et al.* [33], respectively. Based on our modified partial closure definition, as shown in Fig.1, the effective driving force for the fatigue crack propagation, ΔK_{eff}, becomes [3,22-27]:

$$\Delta K_{eff} = K_{max} - K_{min,act} = \Delta K - \Delta K_{sh}\,, \tag{9}$$

where K_{max} and ΔK (= $K_{max} - K_{min}$) are the applied maximum stress intensity factor and stress intensity factor range, respectively.

3. Effect of wedge plasticity in the form of Ramberg-Osgood relationship

Since a variety of artificial closure materials have been introduced into the crack to decelerate or arrest FCP and increase the fatigue life, the plastic deformation of the wedge following Ramberg-Osgood type relationship is further considered in the present study. Then the deformation characteristics of the wedge may be expressed as [34],

$$\varepsilon_1 = \frac{\sigma_1}{E_1} + \left(\frac{\sigma_1}{H}\right)^{\frac{1}{p}}, \tag{10}$$

where p could be called a strain hardening exponent which is applied to the plastic strain term only, H is also a fitting constant. The Ramberg-Osgood equation, unable to be solved explicitly for stress, provides a single smooth/continuous curve for all values of the stress and does not exhibit a well-defined yield point [34]. While the Ramberg-Osgood equation is often used to fit true stress-strain data, it is recently suggested that the fitting based on the engineering stress-strain data provides more accurate description of deformation characteristics [35,36].

As described in [25,27] and shown in Fig.1, during unloading starting from σ_{max}, Eqns (1) and (3) are applicable in stage I prior to the contact of the wedge with the upper fracture surface, and in stage II corresponding to the elastic deformation of the wedge, respectively. In the stage of plastic deformation of the wedge (i.e., stage III) where $\varepsilon_1 > \varepsilon_{1y}$, substituting the following equations [25]:

$$\sigma_1 = \frac{P_1}{t W_1}, \tag{11}$$

$$\varepsilon_1 = 1 - \frac{\delta_1}{h_1}, \tag{12}$$

$$\delta_1 = \sqrt{\frac{a_1}{a_m}}\,\delta\,, \tag{13}$$

into Eqn (10) yields,

$$1 - \frac{1}{h_1}\sqrt{\frac{a_1}{a_m}}\,\delta = \frac{P_1}{tW_1E_1} + \left(\frac{P_1}{tW_1H}\right)^{\frac{1}{p}}. \tag{14}$$

Substituting the following equation [25],

$$\delta = \frac{4Y\sigma}{E'}\sqrt{2aa_m} + \frac{8P_1}{\pi tE'}\sqrt{\frac{a_m}{a_1}}\,, \tag{15}$$

into equation (14), and considering equations (2) and (5) lead to a relationship between the externally applied stress and crack opening displacement,

$$1 - \frac{\delta}{\delta_{op}} = \frac{1}{\lambda_1}\left(\frac{\delta}{\delta_{op}} - \frac{\sigma}{\sigma_{op}}\right) + \left[\frac{E_1}{H\lambda_1}\left(\frac{\delta}{\delta_{op}} - \frac{\sigma}{\sigma_{op}}\right)\right]^{\frac{1}{p}}. \tag{16}$$

Because of the inherent character of the Ramberg-Osgood equation, the externally applied stress cannot be solved explicitly from Eqn (16). A mathematical analysis of Eqn (16) indicates $\frac{d^2\sigma}{d\delta^2} > 0$, thus the σ-δ curve exhibits a concave shape, as shown by stage III in Fig.3.

Stages I, II and III in Fig.3 correspond to Eqns (1), (3) and (16), respectively. It is seen that after the occurrence of plastic deformation of the wedge the slope of the applied stress-COD curve in stage III becomes gradually smaller than that in stage II representing the elastic deformation of the wedge. This signifies that, to bring about a given effective stress range $\Delta\sigma_{eff}$, a smaller externally applied stress range $\Delta\sigma$ (= $\sigma_{max} - \sigma_{min}$) is needed if the wedge plasticity occurs, as shown in Fig.3. In other words, when the applied stress range $\Delta\sigma$ (or the applied minimum stress σ_{min}) remains constant in both cases with and without the wedge plasticity, $\Delta\sigma_{eff}$ becomes larger if the plastic deformation of wedge occurs. This is attributed to the fact that a larger moving space between the crack faces, i.e., a greater ΔCOD experienced by the crack tip becomes available after the occurrence of wedge plasticity. Such a phenomenon of the relaxation or “partial loss” of crack closure effect caused by the plastic deformation of wedge has also been reported in [37]. As a result, the occurrence of wedge plasticity gives rise to a reduction of fatigue crack closure effect.

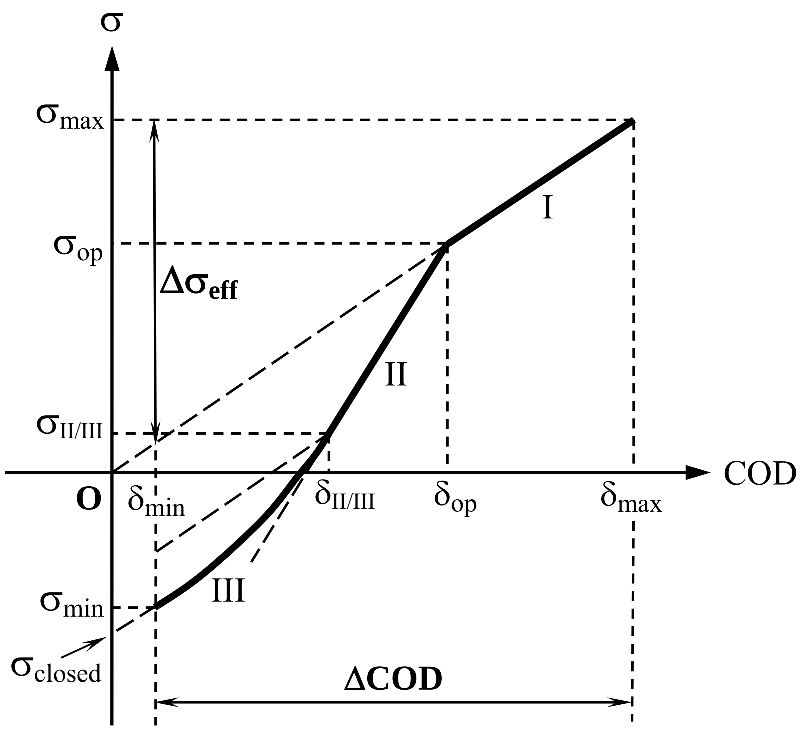

Figure 3 The applied stress-COD behavior for a crack with a wedge exhibiting the plastic deformation in the form of Ramberg-Osgood type relationship (stage I corresponding to closure-free case; stage II corresponding to elastic deformation of the wedge; stage III corresponding to plastic deformation of the wedge), showing the effective stress range ($\Delta\sigma_{eff}$) corresponding to the crack opening displacement range (ΔCOD) experienced by the crack tip.

4. Conclusions

The plastic deformation characteristic of the wedge in the form of Ramberg-Osgood type relationship has been incorporated into the previously proposed elastic wedge closure model and the modified definition of partial fatigue crack closure effect. The analysis indicated that the applied stress-crack opening displacement (COD) response exhibited a non-linear concave variation and its slope became gradually smaller after the plastic deformation of the wedge was taken into consideration. Consequently, a larger COD range would be experienced by the fatigue crack tip, leading to a greater effective stress range. The occurrence of the plastic deformation of the wedge led to a relaxation of the crack tip shielding or closure effect.

Acknowledgements

The financial support provided by the Natural Sciences and Engineering Research Council of Canada (NSERC), Premier's Research Excellence Award (PREA), and Ryerson Research Chair (RRC) programs is gratefully acknowledged.

References

[1] R.H. Christensen, Fatigue crack growth affected by metal fragments wedged between opening-closing crack surfaces, *Appl Mater Res* 2(4) (1963) 207-210.

[2] W. Elber, Fatigue crack closure under cyclic tension, *Eng Fract Mech* 2 (1970) 37-45.

[3] D.L. Chen, B. Weiss, R. Stickler, Z.G. Wang, Brief review and reconsideration of fatigue crack closure effect in materials, *J Mater Sci Tech* 13 (1997) 1-14.

[4] M.N. James, Some unresolved issues with fatigue crack closure - measurement, mechanism and interpretation problems, in: *Advances in Fracture Research (ICF9)*, B.L. Karihaloo, Y.W. Mai, M.I. Ripley and R.O. Ritchie (Eds.), Elsevier Science, Amsterdam, Vol.5, 1997, pp. 2403-2414.

[5] M. Skorupa, Load interaction effects during fatigue crack growth under variable amplitude loading - a literature review. Part II: qualitative interpretation, *Fatigue Fract Eng Mater Struct* 22 (1999) 905-926.

[6] S. Stoychev, D. Kujawski, Methods for crack opening load and crack tip shielding determination: A review, *Fatigue Fract Eng Mater Struct* 26 (2003) 1053-1067.

[7] F.S. Silva, Fatigue crack propagation after overloading and underloading at negative stress ratios, *Inter J Fatigue* 29 (2007) 1757-1771.

[8] C.J. Christopher, M.N. James, E.A. Patterson, K.F. Tee, A quantitative evaluation of fatigue crack shielding forces using photoelasticity, *Eng Fract Mech* 75 (2008) 4190-4199.

[9] L.P. Borrego, J.M. Ferreira, J.M. Costa, Partial crack closure under block loading, *Inter J Fatigue* 30 (2008) 1787-1796.

[10] P.F.P. de Matos, D. Nowell, Numerical simulation of plasticity-induced fatigue crack closure with emphasis on the crack growth scheme: 2D and 3D analyses, *Eng Fract Mech* 75 (2008) 2087-2114.

[11] L.R.F. Rose, C.H. Wang, Self-similar analysis of plasticity-induced closure of small fatigue cracks, *J Mech Phys Solids* 49 (2001) 401-429.

[12] C.H. Wang, L.R.F. Rose, J.C. Newman, Jr., Fatigue crack closure under large-scale yielding conditions, *Fatigue Fract Eng Mater Struct* 25 (2002) 127-139.

[13] P.S. Song, B.C. Sheu, H.H. Chou, Deposition of plating metals to improve crack growth life, *Inter. J. Fatigue* 23 (2001) 259-270.

[14] C.S. Shin, C.Q. Cai, Surface fatigue crack growth suppression in cylindrical rods by artificial infiltration*, Inter J Fatigue* 30 (2008) 560-567.

[15] I. Takahashi, M. Ushijima, C. Takahashi, S. Uematsu, N. Kotani, Automatic restraint and visual detection of fatigue crack growth by applying an alumina paste*, Fatigue Fract Eng Mater Struct* 30 (2007) 832-843.

[16] A.K. Vasudevan, K. Sadananda, Classification of fatigue crack growth behavior, *Metall Mater Trans A* 26A (1995) 1221-1234.

[17] D.A. Lados, D. Apelian, P.C. Paris, J.K. Donald, Closure mechanisms in Al-Si-Mg cast alloys and long-crack to small-crack corrections, *Inter J Fatigue* 27 (2005) 1463-1472.

[18] M.N. James, M.N. Pacey, L.W. Wei, E.A. Patterson, Characterisation of plasticity-induced closure - crack flank contact force versus plastic enclave, *Eng Fract Mech* 70 (2003) 2473-2487.

[19] D. Kujawski, On assumptions associated with ΔK_{eff} and their implications on FCG predictions*, Inter J Fatigue* 27 (2005) 1267-1276.

[20] L.G. Zhao, J. Tong, J. Byrne, The evolution of the stress-strain fields near a fatigue crack tip and plasticity-induced crack closure revisited, *Fatigue Fract Eng Mater Struct* 27 (2004) 19-29.

[21] L.J. Fellows, D. Nowell, Measurement of crack closure after the application of an overload cycle using moire interferometry, *Inter J Fatigue* 27 (2005) 1453-1462.

[22] D.L. Chen, B. Weiss, R. Stickler, A new evaluation procedure for crack closure, *Inter J Fatigue* 13 (1991) 327-331.

[23] D.L. Chen, B. Weiss, R. Stickler, Effect of stress ratio and loading condition on the fatigue threshold, *Inter J Fatigue* 14 (1992) 325-329.

[24] D.L. Chen, B. Weiss, R. Stickler, The effective fatigue threshold - significance of the loading cycle below the crack opening load, *Inter J Fatigue* 16 (1994) 485-491.

[25] D.L. Chen, B. Weiss, R. Stickler, A model for crack closure, *Eng Fract Mech* 53 (1996) 493-509.

[26] D.L. Chen, B. Weiss, R. Stickler, Contribution of the cyclic loading portion below the opening load to fatigue crack growth, *Mater Sci Eng A* 208 (1996) 181-187.

[27] D.L. Chen, Z.Wang, Derivation of applied stress-crack opening displacement relationships for the evaluation of effective stress intensity factor range, *Inter J Fract* 125 (2004) 371-386.

[28] C.S. Shin, Z.Z. Chen, Fatigue life extension by electroless nickel infiltration plating, *Inter J Fatigue* 23 (2001) 777-788.

[29] P.K. Sharp, J.Q. Clayton, G. Clark, Retardation and repair of fatigue cracks by adhesive infiltration *Fatigue Fract Eng Mater Struct* 20 (1997) 605-614.

[30] A. Ur-Rehman, P.F. Thomason, The effect of artificial fatigue-crack closure on fatigue-crack growth, *Fatigue Fract Eng Mater Struct* 16 (1993) 1081-1090.

[31] J.K. Donald, P.C. Paris, Evaluation of ΔK_{eff} estimation procedures on 6061-T6 and 2024-T3 aluminum alloys, *Inter J Fatigue* 21 (1999) S47-S57.

[32] S. Suresh, R.O. Ritchie, Some considerations on the modelling of oxide-induced fatigue crack closure using solutions for a rigid wedge inside a linear elastic crack, *Scripta Metall* 17 (1983) 575-580.

[33] C.J. Beevers, K. Bell, R.L. Carlson, E.A. Starke, A model for fatigue crack closure, *Eng Fract Mech* 19 (1984) 93-100.

[34] N.E. Dowling, *Mechanical behavior of Materials*, 3rd Ed., Pearson Prentice Hall, New Jersey, 2007, pp. 615-622.

[35] Y.J. Kim, N.S. Huh, Y.J. Kim, Y.H. Choi, J.S. Yang, On relevant Ramberg-Osgood fit to engineering nonlinear fracture mechanics analysis, *J Pressure Vessel Tech, Trans ASME* 126 (2004) 277-283.

[36] N.S. Huh, Y.J. Kim, K.B. Yoon, Influence of Ramberg-Osgood fitting on the determination of plastic displacement rates in creep crack growth testing, *Fatigue Fract Eng Mater Struct* 30 (2007) 277-286.

[37] R. Pippan, K. Haberz, H.P. Stüwe, Plastic deformation of fracture surface contacts in fatigue, *Eng Fract Mech* 53 (1996) 441-448.